

## Fractal Dimension Based on Box Counting: A New Parameter for the Quantification of Dynamic PET Studies

Antonia Dimitrakopoulou-Strauss, Ludwig G. Strauss

Medical PET Group - Biological Imaging  
Clinical Cooperation Unit Nuclear Medicine  
German Cancer Research Center, Heidelberg, Germany  
[ads@ads-lgs.com](mailto:ads@ads-lgs.com)

### 1. Introduction

Positron emission tomography (PET) provides the possibility to measure accurately radioactivity concentrations. Standardised uptake values (SUV) have found widespread use since the introduction more than 10 years ago, because it is a fast and reproducible semiquantitative parameter. Some investigators proposed the use of compartmental approaches to obtain more detailed information about the radiopharmaceutical kinetics. However, the application of a two compartment model for the F-18-Deoxyglucose (FDG) kinetics may be limited in some patients, e.g. if the input function is not available or the dynamic data are too noisy. We implemented a non-compartmental method, the fractal dimension, for the analysis of dynamic PET data. In contrast to the two-compartment model, no input function is required. The fractal dimension (FD) is based on the chaos theory and provides information about the “deterministic“ or more “chaotic“ distribution of uptake values. It is a new method, which may be interesting for the evaluation of dynamic data sets like the tracer uptake in an organ as a function of time. While some authors have calculated the FD of an image to assess the bone structure or the distribution of lung ventilation, we applied the FD in the time direction to quantify the FD for each voxel of a dynamic PET study. Purpose of this study was to assess the feasibility and the diagnostic value of the fractal dimension for oncological patient studies, especially in patients following treatment.

### 2. Material and Methods

**Patients:** The evaluation includes 200 tumor lesions (from 159 patients) as well as 57 benign lesions (57 patients). Histologies: 22 metastases from malignant melanoma (17 pretreated patients); four liver metastases from carcinoid tumors (two patients); 29 malignant breast tumors (29 patients); 14 metastases from malignant lymphoma (6 pts with Hodgkin’s disease and one patient with Non-Hodgkin’s disease, following first line treatment); 56 liver metastases (29 patients with metastatic colorectal carcinoma, following first line chemotherapy); 31 malignant bone tumors (10 osteosarcomas, 2 Ewing’s sarcomas, 7 giant cell tumors, one intraosseous hemangiosarcoma, two plasmocytomas, 5 bone metastases, two neuroectodermal tumors, one Non- Hodgkin lymphoma of the bone and one perspiration gland carcinoma); 44 mal. soft tissue tumors (29 liposarcomas, 3 haemangiosarcomas, 6 leiomyosarcomas, 6 mal. fibrous histiocytomas). 101/200 tumors were treated with chemotherapy within the last six months prior to PET.

**Benign lesions:** 2 scars (3 pts) with primary lymphomas, 4 benign breast lesions, 36 benign bone lesions (10 enchondromas, 7 scars, 3 osteomyelitis, 4 bone cysts, two fibromas, two ganglions, one osteitis, one bone necrosis, one bone hematoma, one eosinophilic granuloma, two osteochondroma, one bone edema, one Paget) and 15 benign lesions arising from the soft tissue (7 scars, 5 lipomas, one hemangioma and two inflammatory lesions).

The final diagnosis included the histological data obtained from surgical specimens for the lesions of the musculoskeletal system and the breast lesions, while the clinical follow-up data for at least six months after the FDG study was used for the other patients.

**Data acquisition:** Dynamic PET studies were performed following the application of 300-370 MBq FDG for 60 min. All patients were in fasting state and blood glucose level was measured prior to PET.

A dedicated PET system with a craniocaudal field of view of 15.3 cm was used (theoretical slice thickness 2.4 mm). All PET images were attenuation corrected and reconstructed with a dedicated software package on PC systems using an iterative reconstruction algorithm (weighted least square, ordered subsets).

**Data analysis:** The evaluation of the dynamic PET data was performed using the software package PMod, provided by a cooperation with C. Burger, Univ. of Zuerich, Switzerland. Time-activity curves were created using Volumes of Interest (VOIs). Irregular ROIs were drawn manually. To compensate for possible patient motion during the acquisition time, the original ROIs were visually repositioned, but not redrawn. We used for the basic analysis the semiquantitative approach based on the calculation of a distribution value, for which the term “standardised uptake value” (SUV) was introduced by Strauss and Conti (*The application of PET in oncology. Strauss LG, Conti PS. J Nucl Med 1991;32:623-648*):  $SUV = \text{tissue concentration (MBq/g)} / (\text{injected dose (MBq)} / \text{body weight (g)})$ . The 55-60 minute uptake value was used for the quantification of the data. A non-compartment model based on the fractal dimension was used for the data evaluation. As already shown by other investigators, the fractal dimension is a parameter for the heterogeneity. A Java-based module was implemented in the PMod software to calculate the fractal dimension for the time-activity data. The program is based on the box counting method. Besides the calculation of the FD for VOIs, parametric images of the FD were generated from the dynamic PET data. The statistical evaluation of the data was performed using the Statistica software package (Version 6.0, Stat-Soft Co, Hamburg, Germany). Descriptive statistics and Box-Whiskers plots were used for the analysis of the data. Discriminant analysis was used to determine the diagnostic accuracy using both SUV and fractal dimension with regard to the final histological diagnosis.

### 3. Discussion

PET with FDG is generally used for both the primary diagnosis and staging as well as for follow up in patients after treatment to assess the effect of therapy and/or detect recurrences. Several authors have reported a high sensitivity of FDG PET in untreated patients. We evaluated PET studies in both treated and untreated patients and the quantitative data demonstrated an overlap of the SUV and FD in these patients. Discriminant analysis revealed a low sensitivity of 61% for all lesions, with a sensitivity of 55.6 % for the untreated and 63.4 % for the treated subgroup when the SUV were used to differentiate benign and malignant lesions. The specificity of SUV was high at the level of 91 % for both subgroups. We noted for FD an overall sensitivity of 78 %, with 70.7 % for the untreated and 84.2 % for the treated lesions. The specificity of FD was 72 % for all lesions, 62.5 % for the untreated lesions and 82.1 % for the treated lesions, when FD was used to differentiate benign and malignant lesions. The decision level to discriminate the benign and malignant lesions (calculated by the software) was  $2.3SUV$  ( $tu.:>2.3SUV$ ) and  $1.145FD$  ( $tu.:>1.145FD$ ).

FD was superior to SUV, but the best diagnostic accuracy was achieved when both parameters were used. Interestingly, both SUV and FD had a higher accuracy in treated lesions.

**Conclusions:** The use of FD is a reliable method for the quantification of dynamic PET studies and seems to be more robust than the SUV in particular for the evaluation of treated lesions. It is a fast procedure, which does not demand any input function as compared to compartment methods.

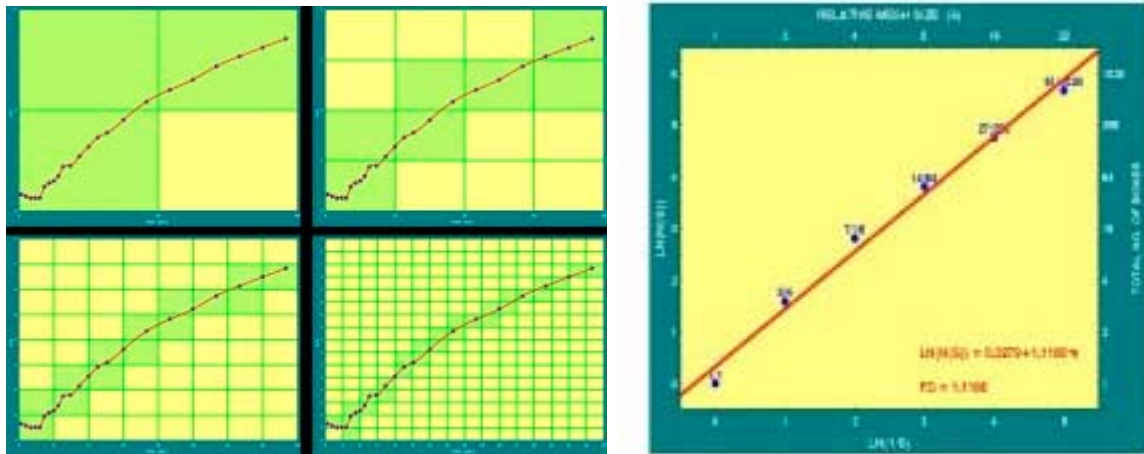


Fig. 1: Calculation of the FD based on box counting method in a time activity curve (TAC) of a giant cell tumor. The TAC of VOI is overlaid with a sequence of rectangular grids. The boxes containing some of the structure of the TAC are highlighted with transparent green.

A log-log plot is generated (number of grid segments, which intersect an object of interest versus the inverse of the grid side length). The slope of a line fitted to the data is used as an estimate of FD (right).

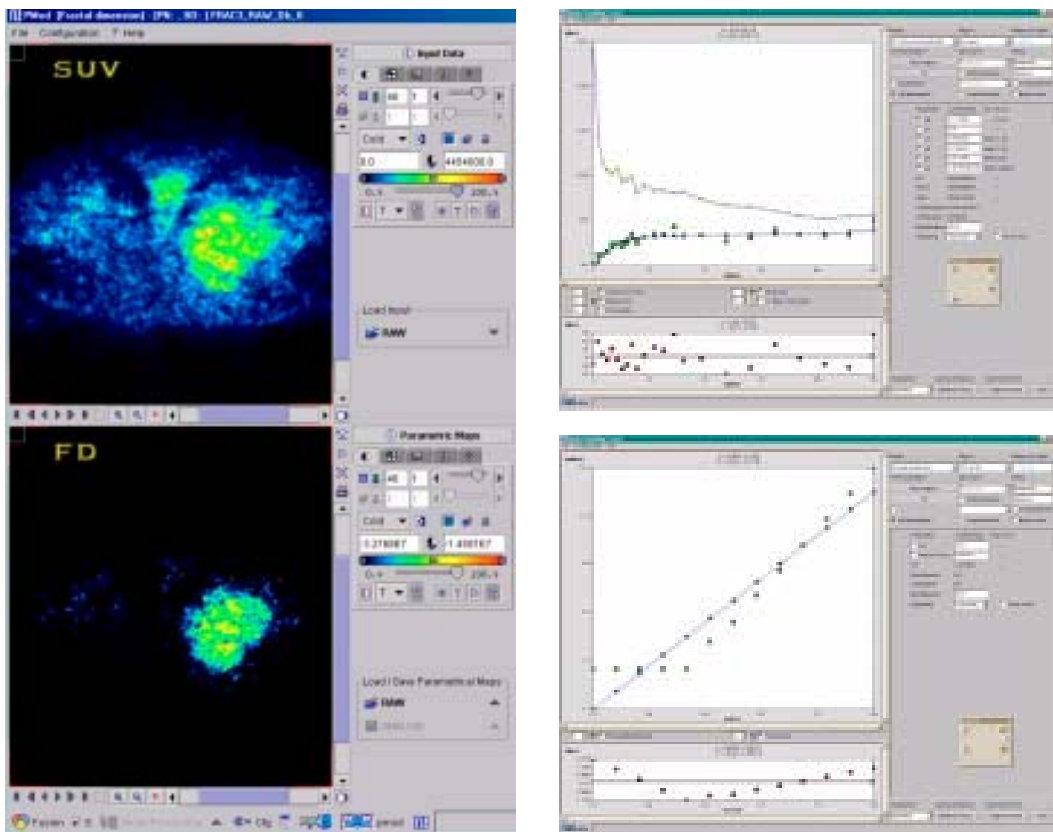


Fig. 2: FDG study of a patient with a soft tissue sarcoma (G I). The SUV image (upper left, SUV) demonstrates tracer uptake in both the tumor and normal structures, while the parametric image of the fractal dimension (lower left, FD) shows only the tumor area. The delineation of the malignant lesion is superior as compared to the SUV image. Upper right: kinetic data for the tumor. Low  $K_1$  and  $k_3$ , resulting in a low tracer uptake. Lower right: calculation of the fractal dimension for the tumor ( $FD=1.41$ ). No input function is needed.

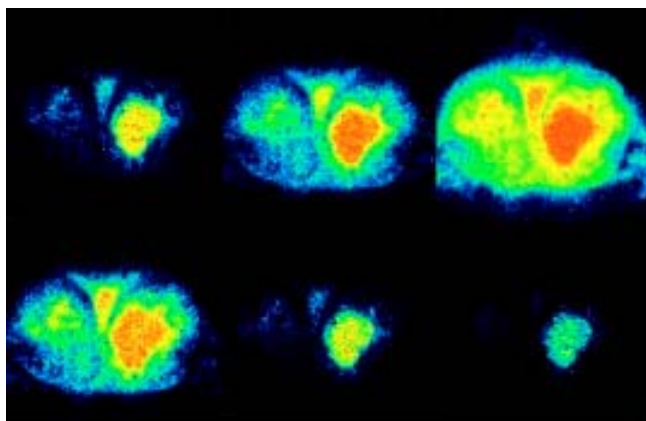


Fig. 3: Pixelwise parametric FD images of the patient in Fig. 2 using different parameters for the FD images. Upper row: the total no. of subdivisions was varied from  $8 \times 8$  (left), to  $32 \times 32$  (middle) to  $128 \times 128$  (right), while the max. was kept constant at 20 SUV. Lower row: constant no. of subdivisions ( $8 \times 8$ ), variation of the max. cutoff SUV from 5 (left) to 30 (middle) to 55 (right).

Tab. 1: Effect of the variation of the number of subdivisions and the cutoff values for the upper threshold on the Minimum and Maximum estimates of FD.

TOTAL NO. BOXES	MAXIMUM (SUV)	MIN FD	MAX FD
$8 \times 8$	<b>20</b>	<b>0.017</b>	<b>0.827</b>
$32 \times 32$	<b>20</b>	<b>0.008</b>	<b>1.084</b>
$128 \times 128$	<b>20</b>	<b>0.005</b>	<b>1.321</b>
$8 \times 8$	<b>50</b>	<b>0.017</b>	<b>1.100</b>
$8 \times 8$	<b>30</b>	<b>0.017</b>	<b>0.629</b>
$8 \times 8$	<b>55</b>	<b>0.017</b>	<b>0.390</b>

Tab. 2: Discriminant analysis for all untreated lesions (99/200) with respect to malignant and benign lesions.

	SUV	FD	SUV, FD
sensitivity	55.55% (55/99)	70.71% (70/99)	58.59% (58/99)
specificity	91.07% (51/56)	62.50% (35/56)	91.07% (51/56)
accuracy	68.39% (106/155)	67.74% (105/155)	70.32% (109/155)
PPV TP	91.66% (55/60)	76.92% (70/91)	92.06% (58/63)
PPV TN	53.68% (51/95)	54.69% (35/64)	55.43% (51/92)

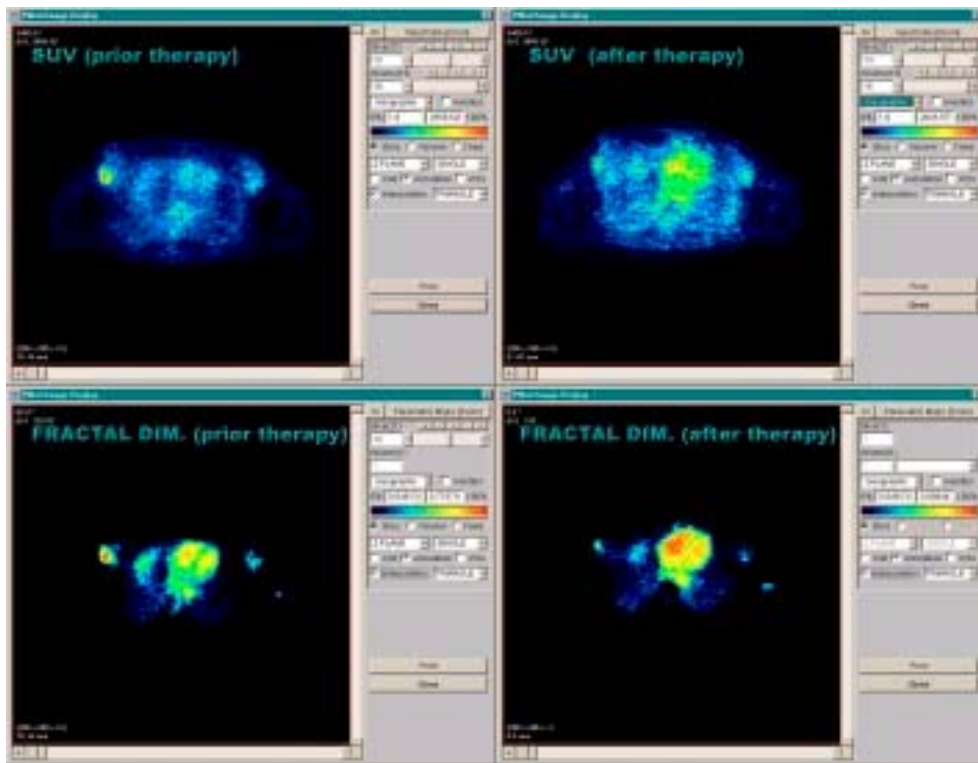


Fig. 4: FDG studies in a patient with a carcinoma of the left and right breast as well as small lung metastases on the right side. The FDG study was performed prior to therapy and one week following high dose chemotherapy. The FDG uptake prior to therapy was highest for the tumor in the right breast (image, upper left). Following treatment we noted a decrease of the tracer uptake (image upper, right; both images are scaled from 0-100 %). The parametric images of the fractal dimension (lower images) delineate both tumors as well as the lung metastases prior and after treatment with high contrast. The fractal dimension was lower following therapy.

Tab. 3: Discriminant analysis for all treated lesions (101/200) with respect to malignant and benign lesions.

	SUV	FD	SUV, FD
sensitivity	63.37% (64/101)	84.16% (85/101)	79.21% (80/101)
specificity	91.07% (51/56)	82.14% (46/56)	83.93% (47/56)
accuracy	73.25% (115/157)	83.44% (131/157)	80.89% (127/157)
PPV TP	92.75% (64/69)	89.47% (85/95)	80.80% (80/99)
PPV TN	57.95% (51/88)	74.19% (46/62)	69.12% (47/68)